HHS Public Access

Author manuscript

Soft Matter. Author manuscript; available in PMC 2016 April 21.

Published in final edited form as:

Soft Matter. 2015 November 7; 11(41): 8165–8178. doi:10.1039/c5sm01143d.

Nano-rheology of hydrogels using direct drive force modulation atomic force microscopy†

Prathima C. Nalam[a], **Nitya N. Gosvami**[a], **Matthew A. Caporizzo**[b], **Russell J. Composto**[b], and **Robert W. Carpick**[a,b]

Robert W. Carpick: carpick@seas.upenn.edu

[a]Department of Mechanical Engineering and Applied Mechanics, University of Pennsylvania, Philadelphia, USA, Fax: +1-215-573-6334; Tel: +1-215-898-4608

[b]Department of Materials Science and Engineering, University of Pennsylvania, Philadelphia, USA

Abstract

We present a magnetic force-based direct drive modulation method to measure local nano-rheological properties of soft materials across a broad frequency range (10 Hz to 2 kHz) using colloid-attached atomic force microscope (AFM) probes in liquid. The direct drive method enables artefact-free measurements over several decades of excitation frequency, and avoids the need to evaluate medium-induced hydrodynamic drag effects. The method was applied to measure the local mechanical properties of polyacrylamide hydrogels. The frequency-dependent storage stiffness, loss stiffness, and loss tangent (tan δ) were quantified for hydrogels having high and low crosslinking densities by measuring the amplitude and the phase response of the cantilever while the colloid was in contact with the hydrogel. The frequency bandwidth was further expanded to lower effective frequencies (0.1 Hz to 10 Hz) by obtaining force–displacement (FD) curves. Slow FD measurements showed a recoverable but highly hysteretic response, with the contact mechanical behaviour dependent on the loading direction: approach curves showed Hertzian behaviour while retraction curves fit the JKR contact mechanics model well into the adhesive regime, after which multiple detachment instabilities occurred. Using small amplitude dynamic modulation to explore faster rates, the load dependence of the storage stiffness transitioned from Hertzian to a dynamic punch-type (constant contact area) model, indicating significant influence of material dissipation coupled with adhesion. Using the appropriate contact model across the full frequency range measured, the storage moduli were found to remain nearly constant until an increase began near ∼100 Hz. The softer gels' storage modulus increased from 7.9 ± 0.4 to 14.5 ± 2.1 kPa (∼85%), and the stiffer gels' storage modulus increased from 16.3 ± 1.1 to 31.7 ± 5.0 kPa (∼95%). This increase at high frequencies may be attributed to a contribution from solvent confinement in the hydrogel (poroelasticity). The storage moduli measured by both macro-rheometry and AFM FD curves were comparable to those measured using the modulation method at their overlapping frequencies (10–25 Hz). In all cases, care was taken to ensure the contact mechanics models were applied within the important limit of small relative deformations. This

†Electronic supplementary information (ESI) available.

Correspondence to: Robert W. Carpick, carpick@seas.upenn.edu.

study thus highlights possible transitions in the probe–material contact mechanical behaviour for soft matter, especially when the applied strain rates and the material relaxation rates become comparable. In particular, at low frequencies, the modulus follows Hertzian contact mechanics, while at high frequencies adhesive contact is well represented by punch-like behaviour. More generally, use of the Hertz model on hydrogels at high loading rates, at high strains, or during the retraction portion of FD curves, leads to significant errors in the calculated moduli.

1. Introduction

Soft matter includes a wide range of natural and synthetic materials including polymeric networks, hydrogels, colloid suspensions, foams, and other biological materials such as cells or tissues. Soft materials are often viscoelastic in nature, and display strain rate dependent mechanical properties. In addition, some soft materials are inhomogeneous and anisotropic, and may have features on multiple length scales resulting in neither ideal solid- nor liquid-like behaviour. Methods to measure the viscoelasticity of macroscopic soft matter samples are well developed. However, nanoscale methods to probe the viscoelastic heterogeneities inherent to soft matter are lacking.

Polymeric hydrogels are one of the most widely used soft materials in biomedical devices,[1–3] sensing platforms,[4,5] artificial tissue scaffolds,[6,7] and drug carriers,[8,9] among other applications. Hydrogels are also frequently used as model surfaces, to study the mechanical properties of biological matter such as cells[10] and tissues.[11,12] This broad set of applications is enabled by the ease of tuning the Young's moduli of the hydrogels from a few kPa[13–15] to a few MPa[16] by varying the crosslinking density of the polymeric network. This spans the range of Young's moduli observed for different cells types and other soft tissues.[17] Further, hydrogels are isotropic and compositionally homogenous, rendering them ideal as well-defined platforms for biological studies.

The optimum functionality of a hydrogel in a specific application strongly depends on appropriate mechanical and rheological properties,[18] especially elastic modulus, strength, and damping. Such properties are highly dependent on the composition of the polymer network[19,20] as well as on their surrounding environment.[21,22] In addition, the mechanical properties of soft materials, due to their viscoelastic nature, can be strong functions of strain, strain rate, and the length scale of the applied strain, among other conditions. Viscoelastic soft materials often possess multiple relaxation times, making it essential to measure the frequency-dependent mechanical response of these materials over a broad range of frequencies. Thus the development of new methodologies is necessary to measure viscoelasticity at the nanoscale and across several frequencies for better understanding of the relevant mechanical properties.

Atomic force microscopy (AFM) is a well-established tool to map the local mechanical properties of soft materials. AFM-based force spectroscopy enables mechanical property measurement across a wide range of forces (typically from pN to μN), time scales, and strains, with nanometer-scale spatial resolution. Modulation techniques can be employed in an AFM to determine the frequency-dependent viscoelastic properties of materials by sensitively measuring or controlling the changes in amplitude and phase of the cantilever

deflection while the tip is in contact with the sample.[23–25] However, the quantitative determination of mechanical properties using AFM is limited by the instrumental noise, creep or drift of the piezo scanners, and the uncertain contact geometries between the AFM probes and the materials being probed.

A lock-in technique for a desired modulation frequency greatly reduces the influence of noise and allows smaller deflections and forces to be measured. However, it is intrinsically difficult to quantify the mechanical behaviour of the contact if the mechanical response of the instrument is non-uniform with drive frequency. Piezoelectric actuation of the cantilever holder or the entire sample is commonly used. However, this generally introduces a forest of spurious peaks due to multiple mechanical resonances of various components, particularly in liquid media, which couple with the actual cantilever response.[26,27] This masks the actual frequency-dependent response of the tip–sample contact. The external environment of soft hydrogels or biological material can significantly influence their mechanical behaviour and hence it is essential to develop methodologies that enable AFM measurements under liquid environment. A direct drive method[26,28–30] using, for example, external electromagnetic forces to actuate the AFM cantilever (also known as Lorentz force microscopy), overcomes this limitation because the excitation is localized just to the free end of the cantilever, eliminating mechanical excitation of other components of the AFM. This enhances the signal-to-noise ratio over a potentially wide frequency range, including on- and off-resonance, enabling high resolution imaging and mechanical property measurements of soft materials under liquid environments.[31] Both normal[26] as well as torsional[32] actuation of the cantilever can be achieved using direct drive methods to map the normal and lateral contact stiffnesses of a heterogeneous sample.

Several studies have used contact resonance force microscopy (CR-FM) methods for a quantitative estimate of the viscoelastic moduli of polymer blends[33,34] and other biological entities.[35] These CR-FM methods measure the viscoelastic properties of material near the resonance frequency of the cantilever which is typically between 25–100 kHz depending on the cantilever stiffness. However, such frequencies are often not biologically relevant. There is a wealth of important processes that occur in biology at frequencies well below the kHz regime. For example, the binding times for actin-crosslinking proteins such as α-actinin or filamin are typically in the range of 0.2–3.0 s (0.3 to 5 Hz[36]), and further at higher frequencies (around few kHz) structural mechanical transitions follow a weak power-law for living cells,[37,38] motivating the need for nano-rheology measurement methods at low frequencies.

To access lower frequencies, off-resonance force modulation atomic force microscopy (FM-AFM) is employed. AFM-based methods to measure the nanoscale viscoelastic properties of soft hydrogels and biological cells are mostly based on modulating the entire sample.[23,24,39–41] For example, Mahaffay *et al.*[10,24] and Radmacher *et al.*[23] measured the viscoelastic response of polymeric hydrogels and cells using a modified piezoelectric scanner which oscillates the sample stage between 20–400 Hz. Igarashi *et al.* extended the modulation frequency up to 20 kHz using a sample stage piezoelectric actuator to determine viscoelastic properties of homopolymers and rubbers.[42] One challenge in these approaches is that one must consider the influence of hydrodynamic drag on the oscillating probe by the

surrounding medium. This drag can confound the measurement of the viscous properties of the sample, and thus must be accounted for when quantifying mechanical properties.[43]

Here, a novel approach using direct drive force modulation AFM was used to explore the dynamic response of hydrogels over a wide frequency range (10–2000 Hz). In our work, we present a novel tip – based direct drive approach, where the modulation force is applied at the tip end of the cantilever, instead actuating the entire sample stage or cantilever chip. Magnetic-based excitation was employed for tip modulation (using the iDrive™ module, Asylum Research, USA) to obtain a stable, artifact-free amplitude and phase response of the cantilever at off-resonant frequencies in an aqueous environment. Since soft materials often have a frequency-dependent response, our methodology is potentially a powerful tool for quantitative determination of the elastic modulus and viscosity of soft materials in liquid environments. Furthermore, a tip-based approach also eliminates the need to estimate of hydrodynamic drag forces acting on the cantilever for appropriate measurement of sample viscosity.[44]

For quantitative assessment of viscoelastic properties using AFM, the contact geometry must be carefully considered. Soft hydrogels undergo large and potentially non-linear strains at relatively low applied forces, especially when probed by a sharp AFM tip.[45,46] When probed with a sharp tip, the sample deformation can easily be much larger than the contact radius, resulting in larger strains (>20%) even at loads as low as 1 pN (shown in the ESI[†]). This violates the assumptions in Hertzian mechanics,[47] the model that is most widely used to calculate the mechanical properties of the soft materials, potentially leading to large errors in calculated moduli (it also violates the assumptions of many other contact mechanics models, some of which are discussed below). Here, we employ spherical silica colloids with an experimentally-measured micrometer-scale radius (∼3 μm) and relatively low roughness (RMS ∼ 2 nm), attached to the end of the cantilever. Although this diminishes spatial resolution, the colloid reduces the applied contact stress and thus the sample deformation compared to sharp AFM tips, and thus presents a well-defined contact geometry to facilitate quantification. These larger probes enable highly compliant materials such as hydrogels to be probed over a much wider range of loads and indentation depths than nanometer-scale probes, while maintaining a contact radius that remains a small fraction of the probe radius, as required for the validity of Hertzian and other contact mechanics model[47] (see ESI,[†] Fig. S2). In particular, we have contact radii typically varying between 10–35% of the tip radius, for the applied loads. Contact probes with radii larger than 3 mm were avoided as a trade-off between spatial resolution and contact deformation. Yoffe proposed a modified Hertz theory for spherical indentation (*i.e.* for contacts with high a/R ratios).[48] For nearly incompressible materials (at Poisson's ratio ∼0.4), such as hydrogels, the error in using the parabolic Hertz model instead of a spherical model at high a/R ratios is less than 1.5%, thus justifying the use of parabolic Hertz contact mechanics in this research (see Fig. S2 in ESI[†]). Finally, the probe tip must have a smooth spherical shape for the Hertz model (and several other models) to apply; colloid roughness in particular can significantly affect the quantitative determination of mechanical properties[49,50] Supporting experiments and analysis along with

[†]Electronic supplementary information (ESI) available.

methodological approaches to address these issues will be described in a future publication.[51]

Thus, this work presents a systematic study to measure the mechanical properties of soft and homogenous[52] polyacrylamide hydrogels across a broad frequency range, from 0.1 Hz to 2 kHz. While force modulation measurements were used to explore the mechanical properties at high frequencies (10 Hz to 2 kHz), slow force–displacement (FD) curves were used for low frequency response measurements. The hydrogel moduli depend on frequency, but the contact mechanical model to describe the system varies from a Hertz-type contact at lower frequencies to a dynamic punch-type model at higher frequency regime. At higher frequencies, the load dependence of the mechanical response shows deviations from the Hertz model, even at low depths of indentation. Specifically, with oscillatory motion of the tip at sufficiently high rates, we hypothesize that the sample does not have time to relax and thus the effect of intrinsic viscoelastic dissipation at the contact interface should be taken into account.

2. Materials and methods

2.1 Preparation of hydrogels

Polyacrylamide gels with two different crosslinking densities were prepared by mixing acrylamide and bis-acrylamide (Sigma-Aldrich, USA) stock solutions at different concentrations as summarized in Table 1. The details of the preparation of polyacrylamide gels are given in ref. 53. Briefly, glass slides, coverslips, and glass boats (vials) were piranha cleaned (70% H_2SO_4 and 30% H_2O_2) for 30 minutes at 80 °C, extensively rinsed with DI water, and then dried in a stream of dry nitrogen. The coverslips were then placed in a glass jar and were silanized *via* vapour deposition using 1 mL of 3-aminopropyltriethoxysilane (APTES) (Sigma-Aldrich, USA) for 2 hours at 80 °C inside a preheated oven. Silanized coverslips were placed in a glass jar containing 0.5 (v/v)% glutaraldehyde solution in PBS solution (Ca^{2+} and Mg^{2+} free, 0.016 M, Fischer, USA) for at least 30 minutes. The glass slides and the boats were placed in a glass jar containing 1 mL of dichlorodimethylsilane (DCDMS) (Sigma-Aldrich, USA) and were silanized for 45 minutes under a continuous nitrogen flow through the jar. Finally, radical polymerization was initiated between the monomer and the crosslinker solution (2 mL) by adding tetramethylethylenediamine (TEMED) (2 μL) (Sigma-Aldrich, USA) and ammonium persulfate (APS) (20 μL, 10 w/v% in PBS) (Sigma-Aldrich, USA) in an eppendorf tube.

Preparation of hydrogels for AFM measurements—A droplet (25 μL) of the polymer mixture was squeezed between the silane-coated glass slide and the coverslip; and the solution was allowed to polymerize for at least 15 minutes. After 15 minutes, the glass slides were removed, and the gels attached to the cover slips were immediately transferred into dishes containing phosphate buffer.

Preparation of hydrogels for macro-rheology measurements—About 1.5 mL of the polymer mixture was pipetted into the silanized boats. The solution in the boat was slowly rotated manually till the bottom of the boat was uniformly covered with the solution, avoiding air bubbles. The polymer mixture was allowed to set for at least for 30–45 minutes

before peeling the gels from the glass boats. The thick gels were also immediately immersed in the phosphate buffer.

The solvent inside the gels was exchanged with fresh PBS buffer at least 2–3 times to remove excess un-crosslinked monomers from the network. Gels were stored in PBS buffer at 4 °C. For measurements, the PBS buffer in the gels was exchanged with DI water by incubating the gels in a dish containing excess of DI water for at least 30 minutes before the use. To avoid substrate effects in the measurements of modulus, samples with large film thicknesses were prepared. The film thicknesses for hydrogels used in AFM and macro-rheology measurement were approximately ∼20 mm and ∼2 mm, respectively. The magnitude of the measured modulus was found to be dependent on the sample age. Such effects were avoided by measuring only on “fresh” samples, *i.e.*, within 5 days after the sample preparation.

2.2 Macro-rheology of hydrogels

Mechanical testing of the hydrogels was performed using a shear rheometer (AR series, TA instruments, New Castle, DE, USA). The rheometer was calibrated for instrumental inertia, air bearing friction, and gap compensation before the measurements. A 20 mm diameter aluminium based parallel-plate configuration was used in the current study. Unsupported polyacrylamide gels were placed on the lower platform (fixed) of the rheometer and the upper plate (movable) was slowly lowered until a small compressive force (∼1–3 N) on the gel was recorded. To avoid slip between the gel and the plate, especially from the thin water film formed from squeezing out of the solvent from the gel, rough emery sheets (Silicon Carbide paper, 240 Grit, South Bay Technology, San Clemente, CA, USA) were glued to the platform and the upper plate using a highly adhesive double-sided tape (Scotch, USA). Shear moduli of the hydrogels were acquired as a function of strain amplitude from 0.5 to 5% at an oscillating frequency of 1 Hz to estimate linear viscoelastic regime for hydrogels. The dynamic storage modulus for hydrogels, measured using the parallel-plate shear rheometer, was found to be independent of strain amplitude until the amplitude exceeded 1%, at which point the storage modulus decreases (Fig. S3, ESI†). Thus, strain amplitude of 0.1% is employed and the frequency dependence response for hydrogels was measured by varying the angular frequency from 0.01–100 Hz with 5 data points measured per decade. The temperature of the system was controlled *via* a thermostat and was held at 24 °C. Dynamic shear moduli (G' and G'') were measured and later translated to normal Young's storage and loss moduli (E' and E'') using a Poisson's ratio of 0.45 for hydrated hydrogels.[15] The experiments were replicated thrice with duplicate repeat measurements on each gel.

2.3 Nano-rheology of hydrogels

Colloid attachment on AFM cantilevers—Silica colloids were attached to the iDrive™ cantilevers (AR-iDrive-N01, Asylum Research, Santa Barbara, USA) using a micromanipulator attached to a long-distance optical microscope (40×, Alessi REL-4100A, NJ, USA). Silicon dioxide microspheres (C-SIO-5.0, diameter ∼5 μm, Microspheres-Nanospheres, Corpuscular, NY, USA) were glued to the cantilevers using two-part epoxy (JB Weld, Sulphur Springs, TXUSA) manipulated by a sharp tungsten wire (TGW0325, World Precision Instruments, Sarasota, FL, USA). The glue was allowed to cure overnight at

room temperature. Reverse imaging of the colloids usually showed debris and other organic contaminants, thus the cantilevers were cleaned in ethanol (Sigma-Aldrich, USA) and then UV-ozone treated (UVO Cleaner model 42, Jelight Co. Inc., Irvine, CA, USA) for at least 15 minutes before use. Colloids with the lowest available RMS roughness (∼1.5–2 nm) were used for viscoelastic measurements.

The colloids' radii were estimated by reverse imaging the colloid-attached cantilevers against a clean test grating (MikroMasch, Spain) which contains tall spikes with sharp ends (∼10 nm radius). The topographic images acquired represent a convolution of tip and sample features. Images with a scan size of 20 μm × 20 μm were acquired in contact mode and at low scan rates (0.5 Hz) to track the curvature of the colloid (ESI†). Image processing and de-convolution of the tip radius was performed using commercial software (Scanning Probe Image Processor (SPIP): Image Metrology, Horsholm, Denmark).

The normal stiffness of the cantilevers was calibrated using thermal noise method[54] using the MFP-3D controller. Thermal noise spectra were acquired in water after attaching the colloids to the cantilevers. The normal deflection sensitivities of the colloid-attached cantilevers were obtained by measuring the slope of FD curves (deflection (d) *vs.* Z sensor position (Z)) on a clean silicon wafer in DI water.

Slow loading measurements—Continuous, slow FD curves, without modulation, were obtained on both hydrogels. FD curves were obtained over a range of constant approach velocities. The maximum depth of indentation for the gels was held at ∼350 nm, well below the calculated contact radii of 1.1 μm. The effective frequencies for the static FD measurements were estimated as the distance travelled by the indenter in the sample (approach and retraction distance) divided by the constant speed of approach of the cantilever.[55,56] This corresponds to a frequency range of 0.1 Hz to 10 Hz when the approach speeds were varied from 100 nm s^{-1} to 8 μm s^{-1}. All measurements were conducted under DI water at a temperature of 22 °C. The elastic moduli were estimated using the contact mechanical fits available in Asylum Research Software, Version AR 12. Approximately 36 FD curves were acquired across different locations on the sample to average the measured mechanical properties. The approach curves were used to estimate the depth of indentation in the hydrogel at an applied force.

Methodology for dynamic modulation measurements—Experiments were conducted using a commercial AFM (MFP-3D, Asylum Research, Santa Barbara, USA) using magnetically-driven iDrive™ cantilevers with normal stiffness of k_n = 0.08–0.1 N m^{-1} and normal resonance frequency of 6–8 kHz. An ARC2 controller with a built-in multi-channel lock-in amplifier was used to record the amplitude and phase response of the cantilever during tip–sample interaction. The cantilevers were actuated in normal mode by applying an AC drive signal though the V-shaped gold-coated (back side) cantilever such that the electromagnetic field generated at the end of the cantilever is perpendicular to the magnetic field generated by an externally attached magnet in the tip holder, inducing forced oscillations (Lorentz force) at the end of the cantilever. The amplitude and the phase response of the cantilever in DI water using piezo actuation (Fig. 1a) and with magnetic actuation using an iDrive™ cantilever (Fig. 1b) show highly contrasting responses. The

'forest of peaks', usually associated with the piezo-driven cantilever due to the vibrations from the mechanical elements in the instrument is eliminated using the iDrive™ cantilever. The resonance frequency obtained (~7.5 kHz) using magnetic actuation closely matches with the response determined from the thermal noise spectrum obtained for the cantilever in liquid medium (not shown). We also observe the first normal mode overtone of the cantilever at 58 kHz. Along with improved signal-to-noise ratio, the direct actuation increases the magnitude of the amplitude both on- and off-resonance, especially before the resonance peak. The spurious peaks in the amplitude and phase signal are still observed at frequencies below 1 kHz using the iDrive™ cantilever and are attributed to the electronic noise from the instrument at these frequencies.

At low modulation frequencies ($f < 1$ kHz), to avoid this electronic noise, a band filter along with appropriate notch filters were used to improve the signal to noise ratio of the cantilever response at each modulating frequency. The notch filters were placed to coincide with output $1f$ and $2f$ signals of the modulating frequency (f) such that the output DC signal from the lock-in is not obscured. The acquisition rate was set to be at least twice the lock-in filter frequency to avoid aliasing. As a result, Fig. 1c in contrast to Fig. 1b, shows a nearly invariant response in amplitude and phase change of the cantilever at off-resonance frequencies (5 Hz to 2 kHz) in aqueous medium. The spurious peaks observed below 1 kHz in Fig. 1b were no longer observed. This frequency-invariant response, especially out of contact, is important for quantitative determination of the frequency dependence of the contact. A similar frequency-invariant response was observed for cantilevers in contact with a silicon wafer.

The dynamic response of the hydrogels were measured by loading the sample in discrete steps. The schematic representation of discrete loading used for dynamic modulation measurements is represented in ESI.† The cantilever was approached from out of contact to a set force with an indentation speed of 4 μm s^{-1} (1 Hz). Note that the approach rate of the indenter in dynamic modulation measurements, unlike the static FD measurements, was held constant for all the measured depths of indentation and modulation frequency. The normal static load on the gel was incremented in discrete steps of 0.5–2 nN for the low cross-linked gel, and 0.5–15 nN for the high crosslinked gels. The approximate depth of indentations obtained in hydrogels varied from 80–350 nm (depending on the applied load).

The drive, corresponding to an out of contact oscillating cantilever amplitude of ~4 nm, was held constant at all frequencies. The amplitude and phase signals were recorded during dwell, and then the tip was retracted from the sample. Data were acquired over a period of 64 seconds at single point of contact (zero scan area) at each fixed depth of indentation. The scan rate was kept slower than the time constants for the lock-in amplifier across all the measured frequencies. The amplitude and phase signals measured as a function of time, at a constant applied force, respectively showed a variation of 0.3 nm and 0.1 degree within the measured window. The drift in the Z-direction, when measured against a hard surface (silicon) was observed to be <0.01 nm s^{-1}. Integral gain used for measurements was optimized such that the change in force with modulation was minimized to <0.03 nN from its mean value, and the drift in the force was held <0.08 nN s^{-1}. Hydrogels showed relaxation within the first 1–2 s of dwell time (ESI†), beyond which the signal was stable

with time. The effect of creep was avoided by neglecting the data acquired in the first few seconds after the dwell period. This discrete or step-wise loading is thus an advantageous approach for excluding creep effects, in contrast with continuous FD measurements. At each measured depth of indentation, the cantilever was modulated at a series of frequencies from 10 Hz to 2 kHz. Both the frequency-dependent and the depth-dependent response of the cantilever were acquired from at least 3 to 4 different locations across the sample. The measurements were further repeated with 2 different tips. The increments in the frequency and load response were randomized. Finally, the storage and loss stiffnesses of the sample were estimated (discussed in the next section) from the recorded amplitude and the phase change signals of the cantilever.

The direct-drive actuation method, in principle, could be used to obtain measurements at even lower frequencies, *i.e.*, below 10 Hz. This is desirable as it would extend the range over which the mechanical spectroscopy is analyzed. However, at lower frequencies, the measurements were more susceptible to $1/f$ noise including the effects of drift leading to unreliable results. Further improvements in the electronics and measuring conditions are currently being investigated to access the lower frequency regime.

3. Theory

3.1 Force modulation response using direct drive AFM

In force modulation measurements, a constant force at the end of the cantilever (F) is applied when the cantilever is out of contact or in contact with the sample. In the out of contact configuration, the force response of the cantilever is represented by a Voigt element as shown in Fig. 2a. When the tip comes in contact with the sample, the oscillating direct drive using the Lorentz force acts directly at the cantilever end, resulting in a parallel arrangement of two Voigt elements: that of the cantilever and that of the contact (Fig. 2b).[25] In Fig. 2, the terms k_n and k_{sample} represent the elastic stiffness of the cantilever and the sample. Similarly, η_o represent the viscosity of the medium while oscillating in a medium, η_{sample} the damping in the viscoelastic sample respectively. At a constant drive, the force at the end of the AFM tip in the direct drive force modulation method is given as:

$$F = A_o e^{i(\omega t+\phi_o)} k_n = A_{sample} e^{i(\omega t+\phi_{sample})}(k_n + k_{sample}) \quad (1)$$

where A_o, A_{sample} are the cantilever deflection amplitudes when the cantilever is out of and in contact with the hydrogel respectively. Similarly, φ_o, φ_{sample} represent the phase difference between the drive signal and the cantilever response when the cantilever is out of contact and in contact with the hydrogel, respectively. The effective stiffness of the sample (k_{sample}) is estimated by rearranging the above equation to obtain:

$$k_{sample} = k_n \left[\frac{A_o e^{i(\omega t+\phi_o)}}{A_{sample} e^{i(\omega t+\phi_{sample})}} - 1 \right]$$

or

$$k_{\text{sample}}=k_{\text{n}}\left[\frac{A_{\text{o}}}{A_{\text{sample}}}(\cos\varphi+i\sin\varphi)-1\right], \quad \text{where } \phi=\phi_{\text{o}}-\phi_{\text{sample}}. \tag{2}$$

Setting $A_o/A_{sample} = \bar{A}$, the storage and loss stiffnesses for the sample can be represented as

$$k'=k_{\text{n}}[\overline{A}\cos\phi-1] \tag{3a}$$

$$k''=k_{\text{n}}\overline{A}\sin\phi \tag{3b}$$

respectively. The dissipation response of the sample compared to its stored energy is the loss tangent, tan δ, where δ is the phase difference between the input signal (φ_o) and the response of the sample (φ_{sample}), *i.e.*

$$\tan\delta=\tan(\phi_{\text{sample}}-\phi_{\text{o}}). \tag{4}$$

Hydrodynamic drag measurements, similar to Navajas *et al.*,[43] were conducted using the colloid probe cantilever on freshly cleaned silicon wafers immersed in DI water at room temperature. Out of contact amplitudes and phase shifts were measured at different distances away from the sample surface and at different modulating frequencies. Especially at high modulating frequencies, a decrease in phase shift with increase in distance between the tip and the sample was observed (not shown). This change in the phase shift with respect to the initial modulation drive signal is associated with the drag on the end of the cantilever from surrounding medium (φ_o), which is a function of both distance and as well the colloid diameter. However, when the cantilever comes in contact with the sample, the corresponding phase shift of the cantilever (φ_{sample}) now includes dissipation from the viscoelasticity of the sample and the drag forces from the surrounding environment near the sample. Thus the contribution to the phase shift from the surrounding medium is accounted and eliminated directly in eqn (2)–(4) by using $\varphi = \varphi_o - \varphi_{Sample}$. Rebelo *et al.*[44] derived equations of motion for the cantilever actuated by a direct drive, while in- and out of contact with the sample. These equations include the inertial retardation effects due to the cantilever mass and the hydrodynamic drag from the medium – by measuring the phase difference of the measured by the cantilever in air (φ_o) and on the sample (φ_{sample}), similar to the ones presented here (eqn (4)).

3.2 Contact mechanical response for linear-elastic materials

The contact mechanics for a sphere-plane contact can be described using the Hertz contact mechanics model.[57] The contact force or load F as a function of the indentation depth (d) is:

$$F=\frac{4}{3}E^{*}R^{1/2}d^{3/2} \tag{5}$$

where R is the radius of the colloid when indented against a flat surface, and $1/E^* = (1 - \nu_{Sample}^2)/E$ where E is the elastic modulus of the sample and ν = Poisson's ratio (the tip is

assumed to be infinitely rigid in comparison to the sample). Note that the power index n for Hertzian contact ($F \propto d^n$) is 1.5. The stiffness of the material (S) as a function of load (F) for a Hertzian contact, using eqn (5) and $S = 2E^*a$, is given by

$$S=(6R)^{\frac{1}{3}}E^{*\frac{2}{3}}F^{\frac{1}{3}} \quad (6)$$

where a is the contact radius for a circular contact, and $a=\sqrt{Rd}$.

The model is not universal: the materials are assumed to be macroscopic, homogeneous, isotropic, linear, and elastic. All strains must be small, *i.e.*, $d \ll a \ll R$, and adhesion is neglected. For significant adhesion, the interfacial energies of the materials must be taken into account using the Johnson–Kendall–Robertson (JKR) model[58] which applies to compliant materials such as hydrogels when indented with tips of sufficiently large radii (such as colloid probes) and sufficiently short-range adhesion. A detailed discussion on the contact mechanics of adhesive materials is provided in the ESI.† The JKR model can be applied to the FD curves using the following equations:

$$\begin{aligned} a^3&=\tfrac{3R}{2E^*}\left(F+6W\pi R+\sqrt{12W\pi R+(6W\pi R)^2}\right)\\ d&=\tfrac{a^2}{R}\left(1-\tfrac{2}{3}\left(\tfrac{a_0}{a}\right)^{\frac{3}{2}}\right)\end{aligned} \quad (7)$$

where W is the work of adhesion and the radius of the contact (a_0) and pull-off forces (F_{adh}) at zero load are represented by

$$\begin{aligned} {a_0}^3&=\tfrac{9\pi R^2W}{2E^*}\\ F_{adh}&=-\tfrac{3}{2}\pi WR\end{aligned} \quad (8)$$

4. Results

4.1 Macro-rheology of polyacrylamide hydrogels

Assuming the hydrogels to be homogenous and isotropic with a Poisson's ratio of 0.45,[15] the storage Young's moduli (E') are estimated from the measured storage shear modulus (G') using macroscopic shear plate rheometry. Fig. 3 shows the storage Young's modulus (E') measured from 0.01 Hz (=0.062 rad s^{-1}) to 50 Hz (=3.1 rad s^{-1}). At higher rotational speeds, beyond 25 Hz, more scatter in the data is observed, attributed to vibrations in the rotating shaft and/or slip at the sample interface. Between 0.01 and 10 Hz, a small increase in the storage modulus is measured for both high- (∼8%) and low- (∼19%) crosslinked gels. The plateau storage moduli (average modulus of the hydrogel between 0.1–10 Hz) for low- and high-crosslinked gels are 5.0 and 17.2 kPa, respectively. The loss tangent values of polyacrylamide gels are represented in ESI,† where the low crosslinked gels exhibit higher loss tangent values in comparison to higher crosslinked gel. A transition is observed, for both the hydrogels, at 10 Hz beyond which an increase in tan δ values is observed with increase in frequency. However, the large error bars associated with both storage modulus

and tan δ values at frequencies beyond 10 Hz, will also include the uncertainties from the instabilities of the instrument operating at such high oscillating frequencies.

4.2 Nano-rheology of polyacrylamide hydrogels

Slow loading measurements—FD curves were obtained by slow linear loading (*i.e.*, with no modulation) of the hydrogels. Representative FD curves obtained at ~0.1 Hz on the low- and high-crosslinked hydrogels using a smooth colloid probe are shown in Fig. 4a. For the approach portion of the slow FD curves, pure repulsion is observed. Polyacrylamide gels which are electrically neutral showed repulsive forces between the colloid and the hydrogel upon contact. Steric repulsive forces with osmotic origin between the loose chain-ends present at the interface of the PAG and the colloid probe under compression dominate and result in negligible adhesion. However once the negatively-charged colloid comes in contact with the hydrogel, the colloid is believed to either interact with the local charges present along the polyacrylamide chains resulting in adhesion and possibly requiring dis-entanglement of chains upon retraction (thus leading to multiple unstable rupture events upon separation).

Repeated FD curves acquired on hydrogels using the colloid probe across the sample presented similar slopes upon contact (estimated error <10%), indicating the absence of colloid contamination from polymer entanglement. Fig. 4b shows representative fits of the approach and retraction curves to the quasi-static FD curves measured at an approach rate of 0.1 Hz. The approach curves showed a good fit to the Hertz model (eqn (5)); except in the initial part curve (first 10′;s of nm). The power index was treated as a free parameter which yielded a value of 1.47 ± 0.40 (yellow line, Fig. 4b). However, the retraction curves, for the hydrogels showed JKR-type behaviour (eqn (7)) showing a direction-dependent contact mechanics behaviour. The fit to the retraction portion (black line, Fig. 4b) was limited to the force at zero indentation depth (dotted line in Fig. 4b); the multiple, long-range rupture events were neglected in this fit. The estimated Young's moduli from quasi-static FD measurements, *i.e.*, using a Hertzian fit for approach and JKR fit for retraction, are provided in Table 2. The different adhesive character of approach vs. retraction for each gel results in Young's moduli slightly higher, but comparable (<15%) during approach (Hertzian fit) in comparison to retraction (JKR). The pull-off force ($F_{\text{pull-off}}$) measured from the JKR fit was used to estimate the effective work of adhesion ($W_{\text{adh,eff}}$) using the relation: $W_{\text{adh,eff}} = F_{\text{pull-off}}/(1.5\pi R)$ (Table 2). The Tabor parameter for high- and low-crosslinked hydrogels were estimated to be ~150 and ~200, respectively, justifying the use of the JKR model for the retraction curves (eqn (S1) in ESI†).

Unlike many materials, hydrogels showed Hertzian behavior on approach curve, while on retract the JKR model fit the data far more closely (Fig. S7, ESI†). In JKR-type materials, the attractive forces between the two surfaces cause spontaneous elastic deformation which increases the contact area until the surface energy is balanced with elastic strain energy. However, our results indicate that these hydrogels do not undergo this spontaneous elastic deformation upon approach. This may be due to the presence of steric repulsion forces of osmatic origin and/or due to negligible long-range attraction forces. Hydrogels being low density polymer structure result in smaller van der Waals forces which are further screened

by the surrounding water. Thus, the load is not affected by interfacial bonding during approach, and the Hertz model applies. We propose that the adhesion only begins to exist when the colloid comes in contact with the hydrogel; upon retraction, these interfacial adhesive bonds resist separation, and the contact follows the JKR model. Polyacrylamide hydrogels in water have shown high polymer–solvent interaction parameter ($\chi \sim 0.5$) resulting in high interactions between the polymer chains and the possibly with the colloid.[59] Such adhesive interactions were observed to significantly reduce when the measurements were performed in PBS solution with ~10 mM NaCl concentration or when the colloid probe was functionalized with neutral dextran molecules (poly-L-lysine-*graft*-dextran). These effects are similar to salting – in effects (lowering χ values) possibly arising from partial hydrolysis of the $-CONH_2$ groups along the polyacrylamide chains.[59] Such adhesion hysteresis, *i.e.*, a different work of adhesion between approach *vs.* retract have been previously reported by Israelachvili *et al.* for several organic systems.[60]

The Young's moduli were measured as a function of approach rates, as shown in the Fig. S8 (ESI†). The depths of indentation for hydrogels were held at ~350 nm and at different approach rates varying from 0.1 Hz to 10 Hz a negligible increase in modulus, similar to macro-rheology measurements, was observed for both high (<9%) and low (~17%) crosslinked gels. The FD curves showed a valid Hertzian fit, even at higher frequencies (~10 Hz), upon approach.

Dynamic modulation studies—Fig. 5 shows the dynamic storage stiffness (k') (eqn (3a)), loss (k'') stiffness (eqn (3b)), and tan δ (eqn (4)) as a function of modulating frequency for high- and low-crosslinked hydrogels. The high crosslinked hydrogels show higher storage stiffness values compared to low crosslinked hydrogels across the entire measured frequency range. As the frequency was varied from 10 Hz to 2 kHz, an approximate 135% and 105% of increase in the storage stiffness was observed for low- and high-crosslinked gels respectively (Fig. 5a).

Both hydrogels show an initial decrease in loss stiffness (up to 100 Hz; the effect being much stronger for the high crosslinked gel) and then a gradual increase with increase in frequency is observed. The loss tangent (Fig. 5b), similar to loss stiffness, reaches a minimum value of approximately 0.01 for both the hydrogel near 100 Hz when compared to values between 0.30–0.15 at the low- and high-frequency ends in the measured frequency ranges. This indicates similar dissipative characteristics of both gels.

Fig. 6 shows the dynamic storage stiffness (estimated using eqn (3a)) as a function of load for the two hydrogels obtained using direct cantilever actuation. The plots show representative storage stiffness data measured at three modulating frequencies: 10 Hz, 500 Hz, and 2000 Hz for both low- (Fig. 6a) and high- (Fig. 6b) crosslinked hydrogels. As the amplitude and phase were obtained by incrementing the normal load on the gel in discrete steps, one would expect that the resulting stiffness–load plots would be comparable to the approach curves obtained using continuous static FD measurements (Fig. 4). However, the Hertz fits (dashed lines) to stiffness–load plots using eqn (6) deviates from the measured data for both gels, particularly more at higher frequencies. The deviations of the Hertz fits from the measured data are represented by the residual errors (%) plotted in Fig. 6. These

ranged from 30 (at low indentation depths) to − 15% (high indentation depths) at 2 kHz. Only at lower modulating frequencies, ∼10 Hz, the Hertzian fit is shown to closely fit the stiffness-load data (residual errors <15%).

5. Discussion

Unlike the non-modulated FD curves (Fig. 4), the stiffness–load curves obtained from dynamic modulation measurements (Fig. 6) deviate from the elastic Hertz model, especially at high modulating frequencies. Greenwood *et al.* showed[61] that adhesive viscoelastic materials can exhibit adhesion hysteresis, *i.e.*, more work is required to separate the surfaces than is gained when creating the contact. Under cyclic loading of viscoelastic or dissipative materials, as in our modulation measurements, the relaxation times for the material may be comparable to the applied modulating frequencies (the relaxation time (creep) for gels was obtained to be ∼0.5–1 s in Fig. S5, ESI†). The contact can thus resist the change in contact area, leading to a "punch-type" mechanical behaviour where the contact area remains constant despite the change in load. Correspondingly, the stiffness (S), which is proportional to the contact radius (a), remains constant. Greenwood defined a non-dimensional parameter ($\bar{\omega}$) for modulation measurements, where $\bar{\omega}=(9\pi/4)^{\frac{1}{3}}(\tau\omega)\mu^2$ describes the transition from elastic contact ($\bar{\omega}<0.1$) to viscoelastic punch-type contact ($\bar{\omega}>5$).[61,62]

The value of $\bar{\omega}$ depends on the modulation frequency (ω), the Tabor parameter μ (*i.e.*, E^*, R, z_o, and W (eqn (S1), ESI†)) and the relaxation time of the material (τ). Our measurements show that PAG gels are reasonably dissipative, with comparable magnitudes for storage and loss stiffnesses observed using the nanoindentation measurements (Fig. 5a). This is further supported by the long relaxation times (τ), 0.5–1.0 s (ESI†), for hydrogels. We calculate $\bar{\omega} \gg 5$ for hydrogels already at low frequencies and thus the punch-type model is applicable for hydrogels. Ebenstein *et al.* describe[55] the frequency-dependent stiffness response, $S(\omega)$, when S is proportional to A (contact area) as

$$S(\omega)=S_0(\omega)\left(\frac{1+\sqrt{1-(F/F_{\mathrm{adh}})}}{2}\right)^{\frac{2}{3}} \quad (9)$$

The values F_{adh} (the adhesion at zero stiffness) and $S_0(\omega)$ (the stiffness at zero load) are determined from fits to stiffness-load data. The fits (Fig. 6, black solid lines) resulted in less than 5% residual error, in contrast with fits of the Hertz model (Fig. 6, black dashed lines), where residual error reached 30%. Thus, the dynamic punch model described the stiffness *vs.* load data more accurately than the Hertz model. The dynamic punch model is shown to fit best at all the explored modulating frequencies, including ∼10 Hz. The Hertzian fit deviates substantially from the measured data even at low indentation depths (Fig. 6), indicating the influence of viscoelasticity on the contact even at small strains. Thus, the deviation from the Hertz model cannot be attributed to high loads (high deformations), but rather, to a dynamic viscoelastic effect. The dynamic storage modulus ($E'(\omega)$) from the stiffness–load curves can be obtained from:[55]

$$E'(\omega)=S_0(\omega)(1-\nu^2)\left(\frac{E^*(0)}{-24RF_{\mathrm{adh}}}\right)^{\frac{1}{3}} \quad (10)$$

where $E^*(0)$ is the reduced relaxation modulus obtained from the Hertz fit to the slow force–distance curves (Fig. 4b). The stiffness–load plots for both hydrogels across all measured frequencies are shown in the ESI.† The dynamic punch model was applied and the values for F_{adh} and S_0 were obtained (eqn (9)) to estimate $E'(\omega)$ at each frequency (eqn (10)). An approximate 35% and 22% increase in $E'(\omega)$ was observed for high-and low-cross-linked hydrogels respectively as the modulation frequency was increased from 10–2000 Hz (Fig. 7 and 8).

Fig. 7 compares the E′ values obtained by applying both dynamic punch model and Hertz model to the force modulation measurements. Regardless of the fitting model used, the storage modulus increases with frequency, showing a viscoelastic stiffening behaviour. For the modulation measurements, the E' values extracted from fitting the Hertz model to the stiffness vs. load data are higher than values extracted from fitting the dynamic punch model. The discrepancy is largest (∼250% and 180% for high- and low-crosslinked gels, respectively) at the highest frequency (2 kHz), and lessens as the frequency reduces thus indicating that the dynamic effects render the dynamic punch model a better fit than Hertz. Although we have not yet been able to extend the dynamic modulation measurements to frequencies below 10 Hz because of drift, collectively the data clearly indicate a transition from Hertzian behaviour at low frequencies to punch-like behaviour at high frequencies occurs around ∼10 Hz. The mechanical moduli values measured from Hertz and dynamic-punch models are found to overlap ∼10–25 Hz (error between the two models <10%) for low crosslinked gel and similarly around ∼10 Hz (error between the two models <30%) for high crosslinked gel. A comparison of the two models for the FD curves measured using slow loading and the dynamic modulation data at 10 Hz showed an insignificant difference (see Fig. S10, ESI†). Thus a clear transition from the elastic – Hertz model to a dissipative dynamic punch model for PAGs occur at ∼10 Hz.

Thus for the dynamic modulation measurements, the dynamic response of the sample acquired while approaching to a desired load can be still be represented by the Hertz model at low frequencies. However, viscoelastic effects begin to manifest at higher frequencies leading to deviation from Hertz-like behavior. Instead, the punch model fits the dynamic modulation measurements for all frequencies. Thus, we propose that it is important to consider the loading history (*i.e.*, adhesion hysteresis seen between approach and retract) and the loading frequency (viscoelasticity) before applying contact mechanics to analyze the material. Failing to take these issues into account may lead to large errors in extracted values of the modulus for example.

Comparisons of the storage moduli measured across 4 decades of frequency space using different length scale of measurement, *i.e.*, nanoscale static FD measurements (applying the Hertz fit to extract E'), nanoscale modulation measurements (applying the punch fit to extract E'), and macroscale parallel-plate rheology measurements are presented in Fig. 8.

Note that the nano-rheology moduli presented in Fig. 8 are the average values of storage moduli obtained using two different tips (ESI†).

The values obtained from slow FD measurements are consistent with the values obtained from the dynamic punch model fits in forming a smooth increasing trend of E' *vs.* frequency. While the static indentation measurements are effectively a non-sinusoidal modulation with large amplitude (∼depth of indentation), the dynamic modulation measurements are a sinusoidal modulation with small amplitude employed at a fixed depths of indentation. However, similar storage modulus for hydrogels are obtained from different approaches (by employing appropriate contact mechanical models) which indicate the fact that the frequency response of the storage modulus is a time-dependent (viscoelastic) effect, and is independent of the amplitude of the modulation.

Further, the E' values extracted from macro-rheology measurements agree reasonably well, within the experimental error, with both slow FD and the dynamic modulation measurements across the overlapping frequency space. There are several differences between the different scales of experiments such as: the length scale of the applied strain and the measured responses; the nature of the imposed stress state; and the presence of surface effects in the nano-rheology measurement. Despite this, the agreement in elastic moduli values indicates a negligible scale effect on mechanical properties of the hydrogel. This comparison of the mechanical properties of hydrogels, using different techniques across a broad frequency range, is presented here for the first time. The reasonable agreement using different modes of measurements also indicates the appropriateness of the dynamic punch model for the modulation measurements. Storage moduli showed an approximate ∼95% and ∼80% increase for high- and low-crosslinked hydrogels when the frequencies were increased from 0.1 Hz to 2000 Hz.

The non-monotonic dependence of the loss tangent on frequency is observed for both macro- and nano-scale measurements (Fig. S12, ESI†). Overall, both gels have similar magnitudes of tan δ at the low- (10 Hz) and high-frequency (2 kHz) ends of the measured frequency ranges, reaching minimum values near 100 Hz for nano scale measurements. However, in contrast to the AFM measurements, the minimum dissipation occurs near 10 Hz in macro-rheology measurements. Thus, unlike the storage moduli, a substantial difference is observed for loss tangent values obtained from the nano- and macro-rheology measurements. This indicates that the dissipative losses are more sensitive to the scale of measurement. These disparities can be attributed to multiple factors including surface effects (present only in the nanoscale measurements), different volumes of material being probed, and the very different stress states involved (pure shear for the rheometer, *versus* a heterogeneous stress state dominated by compression for the AFM). Such effects need further investigation, which is beyond the scope of the current paper.

Fig. 8 shows a plateau at low frequencies (∼up to 50–100 Hz) for both the hydrogels. Such a plateau is also observed in other force modulation studies of hydrogels.[10] However, beyond this transition frequency, an increase in E' is observed for both low-and high-cross-linked gels demonstrating significant frequency effects on the gels' mechanical responses. The frequency-dependent mechanical response for biphasic structures, under mechanical

compression can be attributed mainly to two phenomena: viscoelasticity and poroelasticity of gels. While viscoelasticity results from the relaxation of polymer chains between entanglements, poroelasticity results from the diffusion of solvent through the porous polymer network. The two processes can result in a complex time-dependent mechanical behaviour for hydrogels that can lead to the observed stiffening with increase in frequency.

Polyacrylamide gels are made by chemically crosslinking acrylamide (monomer) with bis-acrylamide (crosslinker) to form a crosslinked elastic network. This network resists the rearrangement of crosslinkers, unlike that seen for ionically crosslinked gels, in the presence of external applied load, resulting in stress relaxation mainly through migration of water.[63] Dissipation due to flow-dependent poroelasticity depends on the characteristic contact length scales ($a = \sqrt{Rd}$) and the effective diffusivity (D) of the solvent through the network ($\tau_{poro} = a^2/D$). Kalcioglu *et al.*[64] recently probed the poroelastic relaxation times for polyacrylamide gels at both macro- and micro-scales at different indentation depths. While the diffusion constants remained almost invariant, several orders of decrease in τ_{poro} was observed as the contact length scales were reduced. Using a similar diffusion constant ($D \sim 2 \times 10^{-10}$ m s^{-2}) the τ_{poro} for PAG gels in our contact geometries ($R \sim 4.5$ μm and depth of indentation ∼500 nm) were ∼0.01 s ($f \sim 100$ Hz) indicating that diffusion is fast relative to the characteristic length scale.

Thus in Fig. 8, at lower frequencies, we propose that the gel behaves as a relaxed elastic solid with complete migration of solvent in and out of the network during load cycling.[65] The relaxation processes, such as motions of chain segments between cross-links, are relatively slow, resulting in nearly frequency-independent moduli at lower frequencies. However, when the modulating frequencies are comparable to the poroelastic relaxation times ($f \sim 100$ Hz), it becomes harder for the solvent to migrate in and out of the network, increasing the stiffness of the gel and hence the storage moduli (as seen in Fig. 8 starting at ∼ 50–100 Hz). The transition in tan δ (Fig. 5b) at $f \sim 100$ Hz also might be attributable to this transition from an elastic solid without entrapped water to a gel with entrapped water. The dissipative contribution from both the rearrangement of polymeric network or from the diffusion of the solvent molecules through the network coupled with adhesion between the tip and sample can result in the contact area remaining constant as the load is cycled at small amplitudes. Thus, unlike elastic contact mechanics models such as the Hertz and JKR models where the contact area is changing during cycling, the dynamic punch model (constant contact area during cycling) more accurately captures the viscoelastic behaviour observed in these polyacrylamide gels and, correspondingly, leads to a more accurate determination of the moduli.

6. Conclusions

Soft materials, such as hydrogels and cells, often exhibit frequency-dependent mechanical properties. Since the mechano-sensing processes in biological materials, and the relaxation processes in polymers and gels often occur at low strain rates, we developed a direct drive, force modulation technique using magnetic actuation of a colloid-attached cantilever. As opposed to sample or cantilever chip drive, the direct-drive method modulates the free end of the cantilever (at the tip). Off-resonance frequencies of the cantilever were exploited to

measure the mechanical properties over a range of frequencies (nearly 3 decades) without measurement artefacts. Further, this method eliminates the necessity of estimating the drag forces between tip and sample. The method was employed to measure the frequency-dependent mechanical response of model polyacrylamide hydrogels. Care was taken to ensure that indentations were small compared to the tip radius, an important condition for the contact mechanics models to be accurate. We measured the viscoelastic response of polyacrylamide hydrogels across a broad range of frequencies (0.1 Hz to 2 kHz) which enabled us to observe different mechanical regimes for hydrogels. Nanoscale measurements, were obtained *via* FD curves under slow loading (0.1 Hz to 10 Hz) and using a direct drive modulation technique (10 Hz to 2 kHz).

The FD curves acquired with a slow loading rate exhibited a direction-dependent contact mechanical response. While a repulsive, Hertzian-type contact behaviour was observed on approach, substantial tensile forces were needed to separate the contact due to adhesion, resulting in JKR-type contact mechanics for the retraction. The dynamic modulation measurements showed comparable magnitudes for the storage and loss stiffness, demonstrating a significant dissipative nature of the hydrogel networks. A transition from Hertzian behaviour at low frequencies (below 10 Hz) to punch-like behaviour at high frequencies (above 25 Hz) is observed. Applying the Hertz model at higher frequencies fails to fit stiffness *vs*. load data and significantly overestimates the Young's modulus. In contrast, the dynamic punch model fit the stiffness *vs*. load data extremely well for all the measured frequencies and depths of indentation. The storage modulus showed a distinct ∼95% and ∼80% increase for high- and low-crosslinked hydrogel. We propose that the increase in modulus with frequency above ∼100 Hz reflects a stiffening of the mechanical response due to solvent confinement in the hydrogel.

Further, different loading approaches commonly used in the literature to measure the viscoelastic properties of soft materials were compared. The measured moduli are indeed highly dependent on the frequency of the applied load but not on the amplitude of the modulation. The novel measurement method presented here, coupled with proper analysis, thus opens up the possibility of using nanoscale viscoelastic spectroscopy to measure the relevant mechanical properties of soft matter generally, and to distinguish between different states of soft matter. The approach has potential for application to biological materials such as tissues and cells and to detect changes, *e.g.*, due to diseased or stressed states.

Supplementary Material

Refer to Web version on PubMed Central for supplementary material.

Acknowledgments

The authors thank Mr Anil Gannepalli from Asylum Research, USA for help with AFM instrumentation and as well for generously loaning us the iDrive™ Lorentzian actuated cantilever holder. The authors also thank the Nano/Bio Interface Centre at the University of Pennsylvania for use of instrumentation. We would like to thank Prof. David M. Eckmann (DE), Department of Anaesthesiology and Critical Care, University of Pennsylvania for useful discussions and Prof. Jason Burdick, Chris Rodell from Department of Biomedical Engineering, UPenn for the access to the TA macro-rheometer. The authors would also like to thank Mr Luke Villermin for his contribution in designing the table of contents image. This research was partially supported by the Nano/Bio Interface Centre through the National Science Foundation NSEC DMR08-32802 (RC, RJC, DE), Office of Naval Research grant

N000141410538 (DE) and Swiss National Science Foundation (SNF). RJC acknowledges partial support from NSF Polymers Program through DMR09-07493.

Notes and references

1. Peppas NA, Hilt JZ, Khademhosseini A, Langer R. Adv Mater. 2006; 18:1345–1360.
2. Hoffman AS. Adv Drug Delivery Rev. 2002; 54:3–12.
3. Gaharwar AK, Peppas NA, Khademhosseini A. Biotechnol Bioeng. 2014; 111:441–453. [PubMed: 24264728]
4. Gawel K, Barriet D, Sletmoen M, Stokke BT. Sensors. 2010; 10:4381–4409. [PubMed: 22399885]
5. Khimji I, Kelly EY, Helwa Y, Hoang M, Liu J. Methods. 2013; 64:292–298. [PubMed: 23978515]
6. Geckil H, Xu F, Zhang XH, Moon S, Demirci U. Nanomedicine. 2010; 5:469–484. [PubMed: 20394538]
7. Moreira-Teixeira L, Jin R, Dijkstra P, Feijen J, van Blitterswijk C, Karperien M. Tissue Eng, Part A. 2008; 14:711.
8. Vashist A, Vashist A, Gupta YK, Ahmad S. J Mater Chem B. 2014; 2:147–166.
9. Schmidt JJ, Rowley J, Kong HJ. J Biomed Mater Res, Part A. 2008; 87:1113–1122.
10. Mahaffy RE, Shih CK, MacKintosh FC, Kas J. Phys Rev Lett. 2000; 85:880–883. [PubMed: 10991422]
11. Stolz M, Raiteri R, Daniels AU, VanLandingham MR, Baschong W, Aebi U. Biophys J. 2004; 86:3269–3283. [PubMed: 15111440]
12. McKee CT, Last JA, Russell P, Murphy CJ. Tissue Eng, Part B. 2011; 17:155–164.
13. Engler A, Bacakova L, Newman C, Hategan A, Griffin M, Discher D. Biophys J. 2004; 86:388a.
14. Engler AJ, Richert L, Wong JY, Picart C, Discher DE. Surf Sci. 2004; 570:142–154.
15. Boudou T, Ohayon J, Picart C, Tracqui P. Biorheology. 2006; 43:721–728. [PubMed: 17148855]
16. Stammen JA, Williams S, Ku DN, Guldberg RE. Biomaterials. 2001; 22:799–806. [PubMed: 11246948]
17. Alonso JL, Goldmann WH. Life Sci. 2003; 72:2553–2560. [PubMed: 12672501]
18. Engler AJ, Sen S, Sweeney HL, Discher DE. Cell. 2006; 126:677–689. [PubMed: 16923388]
19. Gong JP, Katsuyama Y, Kurokawa T, Osada Y. Adv Mater. 2003; 15:1155.
20. Sun JY, Zhao XH, Illeperuma WRK, Chaudhuri O, Oh KH, Mooney DJ, Vlassak JJ, Suo ZG. Nature. 2012; 489:133–136. [PubMed: 22955625]
21. Johnson BD, Beebe DJ, Crone W. Mater Sci Eng, C. 2004; 24:575–581.
22. Qiu Y, Park K. Adv Drug Delivery Rev. 2001; 53:321–339.
23. Radmacher M, Tilmann RW, Gaub HE. Biophys J. 1993; 64:735–742. [PubMed: 19431876]
24. Mahaffy RE, Park S, Gerde E, Kas J, Shih CK. Biophys J. 2004; 86:1777–1793. [PubMed: 14990504]
25. Florin EL, Radmacher M, Fleck B, Gaub HE. Rev Sci Instrum. 1994; 65:639–643.
26. Xu X, Koslowski M, Raman A. J Appl Phys. 2012; 111:054303.
27. Schaffer TE, Cleveland JP, Ohnesorge F, Walters DA, Hansma PK. J Appl Phys. 1996; 80:3622–3627.
28. Han WH, Lindsay SM, Jing TW. Appl Phys Lett. 1996; 69:4111–4113.
29. Hoof S, Gosvami NN, Hoogenboom BW. J Appl Phys. 2012; 112:114324.
30. Jarvis SP, Ishida T, Uchihashi T, Nakayama Y, Tokumoto H. Appl Phys A: Mater Sci Process. 2001; 72:S129–S132.
31. Ge GL, Han D, Lin DY, Chu WG, Sun YX, Jiang L, Ma WY, Wang C. Ultramicroscopy. 2007; 107:299–307. [PubMed: 17045399]
32. Gosvami NN, Nalam PC, Exarhos AL, Tam QZ, Kikkawa JM, Carpick RW. Appl Phys Lett. 2014; 105:093101.
33. Yuya PA, Hurley DC, Turner JA. J Appl Phys. 2008; 104:074916.

34. Killgore JP, Yablon DG, Tsou AH, Gannepalli A, Yuya PA, Turner JA, Proksch R, Hurley DC. Langmuir. 2011; 27:13983–13987. [PubMed: 22054300]
35. Cartagena A, Hernando-Perez M, Carrascosa JL, de Pablo PJ, Raman A. Nanoscale. 2013; 5:4729–4736. [PubMed: 23598736]
36. Wottawah F, Schinkinger S, Lincoln B, Ananthakrishnan R, Romeyke M, Guck J, Kas J. Phys Rev Lett. 2005; 94:098103. [PubMed: 15784006]
37. Smith BA, Tolloczko B, Martin JG, Grutter P. Biophys J. 2005; 88:2994–3007. [PubMed: 15665124]
38. Fabry B, Maksym GN, Butler JP, Glogauer M, Navajas D, Taback NA, Millet EJ, Fredberg JJ. Phys Rev E: Stat, Nonlinear, Soft Matter Phys. 2003; 68:041914.
39. Park S, Koch D, Cardenas R, Kas J, Shih CK. Biophys J. 2005; 89:4330–4342. [PubMed: 16199496]
40. Nia HT, Bozchalooi IS, Li Y, Han L, Hung HH, Frank E, Youcef-Toumi K, Ortiz C, Grodzinsky A. Biophys J. 2013; 104:1529–1537. [PubMed: 23561529]
41. Alcaraz J, Buscemi L, Grabulosa M, Trepat X, Fabry B, Farre R, Navajas D. Biophys J. 2003; 84:2071–2079. [PubMed: 12609908]
42. Igarashi T, Fujinami S, Nishi T, Asao N, Nakajima K. Macromolecules. 2013; 46:1916–1922.
43. Alcaraz J, Buscemi L, Puig-de-Morales M, Colchero J, Baro A, Navajas D. Langmuir. 2002; 18:716–721.
44. Rebelo LM, de Sousa JS, Mendes J, Schape J, Doschke H, Radmacher M. Soft Matter. 2014; 10:2141–2149. [PubMed: 24651941]
45. Dimitriadis EK, Horkay F, Maresca J, Kachar B, Chadwick RS. Biophys J. 2002; 82:2798–2810. [PubMed: 11964265]
46. Lin DC, Horkay F. Soft Matter. 2008; 4:669–682.
47. Hertz, HR. Ueber die Beruehrung elastischer Koerper (On Contact Between Elastic Bodies), in Gesammelte Werke (Collected Works). Vol. 1. Leipzig, Germany: 1882. 1895
48. Yoffe EH. Philos Mag A. 1984; 50:813–828.
49. Buzio R, Valbusa U. J Phys: Condens Matter. 2008; 20:354014.
50. Jacobs TDB, Ryan KE, Keating PL, Grierson DS, Lefever JA, Turner KT, Harrison JA, Carpick RW. Tribol Lett. 2013; 50:81–93.
51. P. C. Nalam, L. Villermin, R. J. Composto and R. W. Carpick, 2015, to be submitted
52. Flores-Merino MV, Chirasatitsin S, LoPresti C, Reilly GC, Battaglia G, Engler AJ. Soft Matter. 2010; 6:4466–4470. [PubMed: 20953281]
53. Tse JR, Engler J. Curr Protoc Cell Biol. 2010 unit 10.16.
54. Hutter JL, Bechhoefer J. Rev Sci Instrum. 1993; 64:1868–1873.
55. Ebenstein DM, Wahl KJ. J Colloid Interface Sci. 2006; 298:652–662. [PubMed: 16455101]
56. Ren J, Yu SY, Gao N, Zou QZ. Phys Rev E: Stat, Nonlinear, Soft Matter Phys. 2013; 88:052711.
57. Johnson, KL. Contact Mechanics. Cambridge University Press; Cambridge: 1985.
58. Johnson KL, Kendall K, Roberts AD. Proc R Soc London, Ser A. 1971; 324:301–313.
59. Sivanantham M, Tata BVR. Pramana J Phys. 2012; 79:457–469.
60. Yamada S, Israelachvili J. J Phys Chem B. 1998; 102:234–244.
61. Greenwood JA, Johnson KL. J Colloid Interface Sci. 2006; 296:284–291. [PubMed: 16203010]
62. Wahl KJ, Asif SAS, Greenwood JA, Johnson KL. J Colloid Interface Sci. 2006; 296:178–188. [PubMed: 16168427]
63. Zhao XH, Huebsch N, Mooney DJ, Suo ZG. J Appl Phys. 2010; 107:063509.
64. Kalcioglu ZI, Mahmoodian R, Hu YH, Suo ZG, Van Vliet KJ. Soft Matter. 2012; 8:3393–3398.
65. Hu YH, Suo ZG. Acta Mech Solida Sin. 2012; 25:441–458.

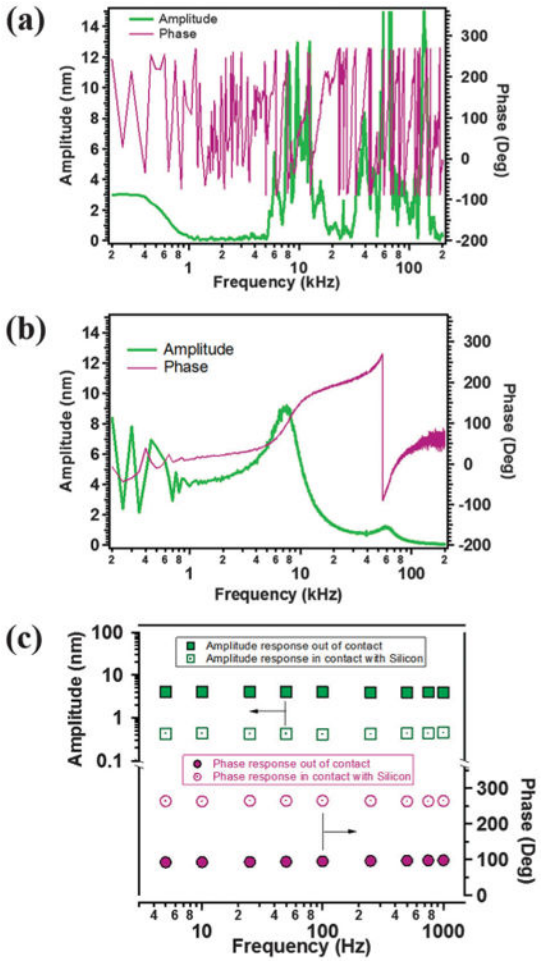

Fig. 1.

The amplitude and phase response of a cantilever (colloid attached, k_n = 0.068 N m^{-1}) as a function of frequency. The response of the cantilever with (a) piezo actuation and (b) magnetic actuation (using iDrive™) are shown. Resonant frequency of the cantilever was measured at ∼7.5 kHz. (c) The response of the magnetically-actuated AFM cantilever at off-resonance frequencies (5 Hz to 2 kHz), after adding appropriate filters, is shown when oscillating the cantilever out of contact (closed symbols) and in contact with a silicon wafer (open symbols) in DI water.

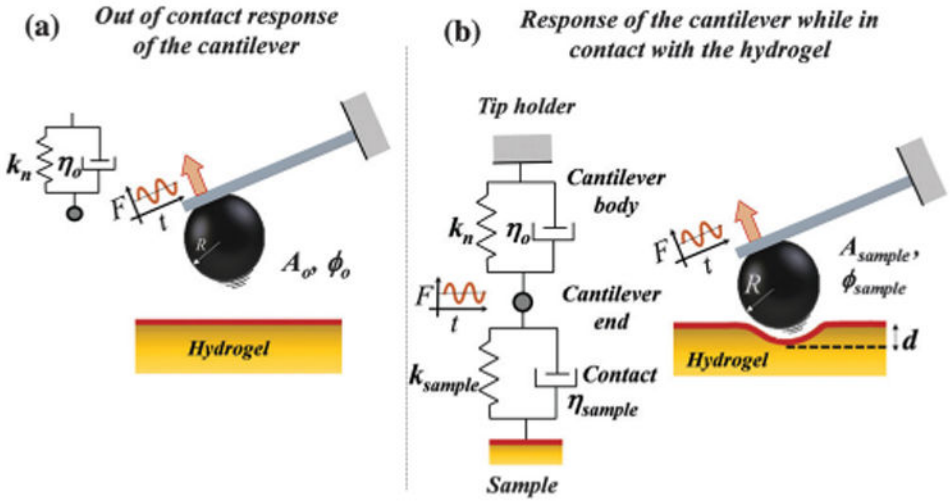

Fig. 2.

Schematic representation of the response of colloid-attached, oscillating cantilever (a) out of contact and (b) in contact with hydrogel (sample) is shown.

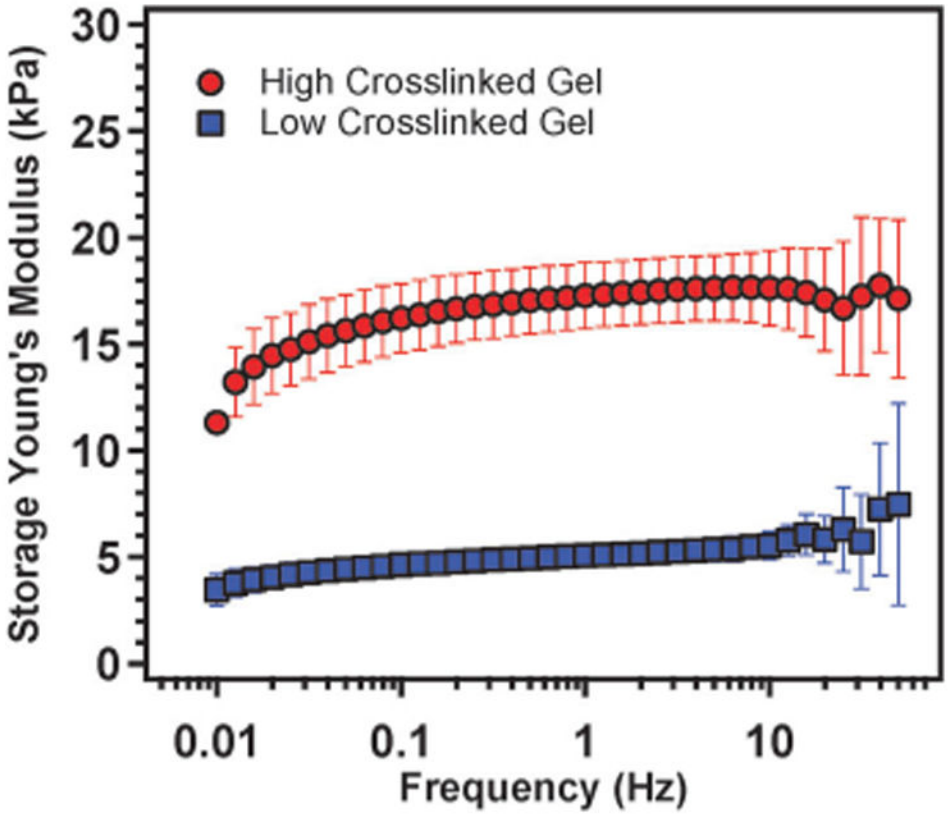

Fig. 3.

The storage Young's modulus (E') as a function of frequency obtained from parallel-plate rheometer for high- (red, circles) and low-(blue, squares) crosslinked polyacrylamide hydrogels. Applied strain = 0.1%, temperature = 24 °C.

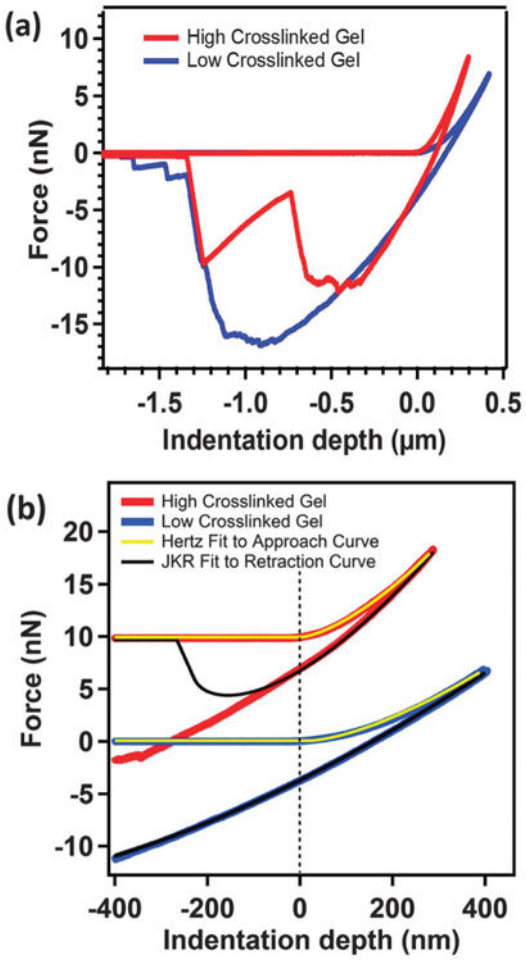

Fig. 4.

(a) The representative FD curves measured on low (blue)- and high (red)-crosslinked polyacrylamide hydrogels in DI water. (b) Representative Hertz fit (yellow) and JKR fit (black) to approach and retraction curves, respectively. Cantilever stiffness = 0.098 N m^{-1}, approach and retract velocity = 100 nm s^{-1}.

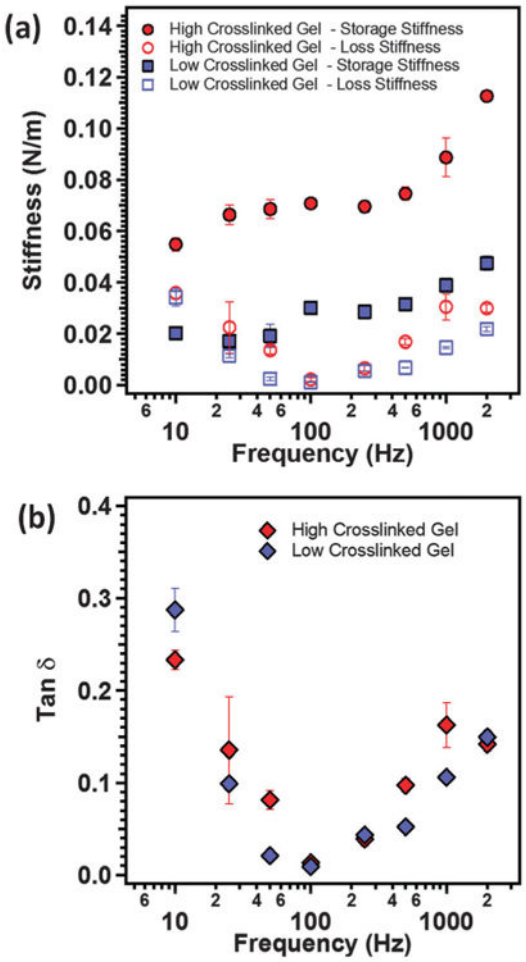

Fig. 5.

(a) The storage modulus (closed symbols), loss modulus (open symbols) and (b) tan δ as function of modulation frequency of the AFM cantilever for polyacrylamide gels with two different crosslinking densities.

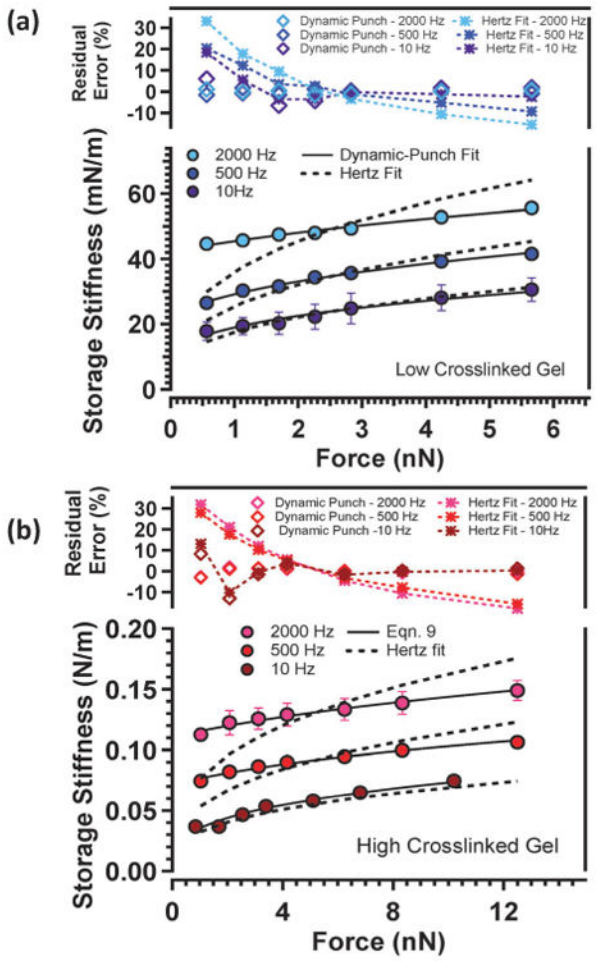

Fig. 6.

Force-dependent response of storage stiffness for (a) low- and (b) high-crosslinked polyacrylamide hydrogels at three representative modulating frequencies of 10 Hz, 500 Hz and 200 Hz. The fits and the corresponding residual errors (%) from the Hertz and dynamic punch model are also shown.

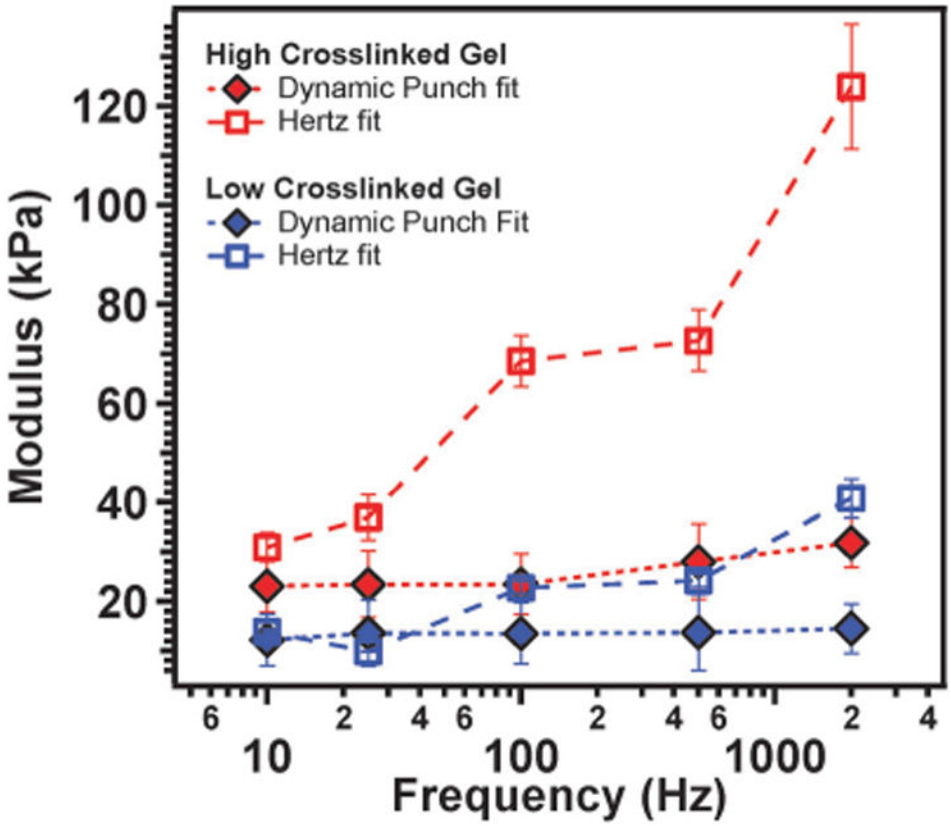

Fig. 7.

The elastic moduli of low- and high-crosslinked hydrogels (blue and red respectively) obtained from dynamic modulation measurements calculated using Hertz (open symbols) and dynamic punch (closed symbols) fits.

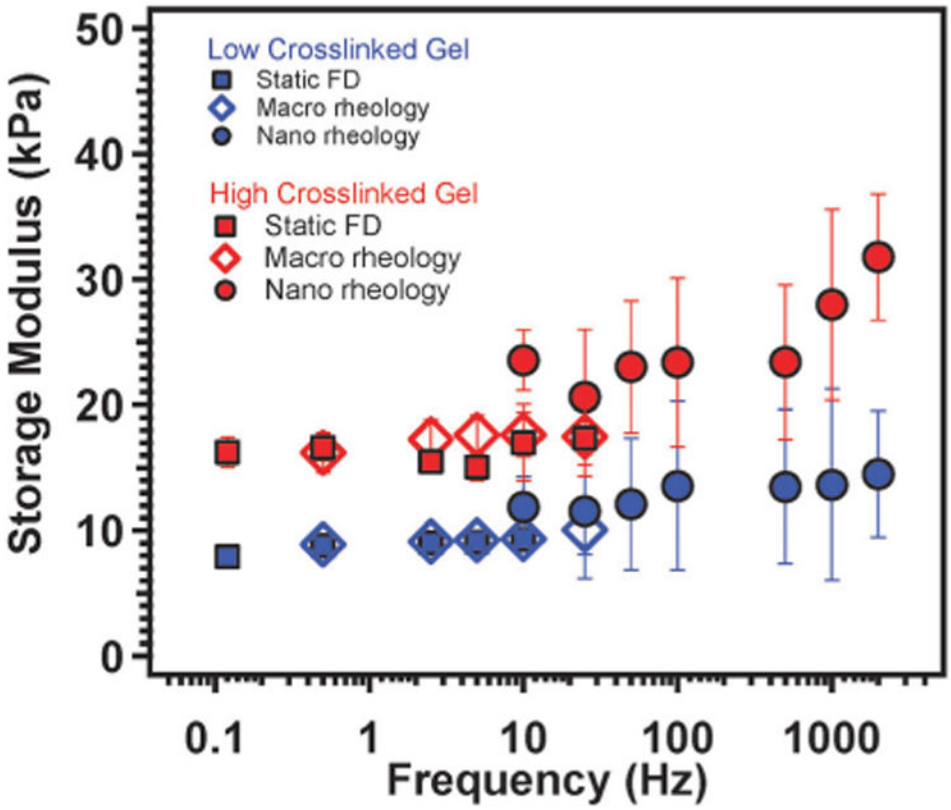

Fig. 8.

Comparing the storage elastic modulus E' of the low- (blue) and high-(red) polyacrylamide gels measured using nano-scale static FD curves (AFM, closed squares), nano-scale dynamic modulation (AFM, closed circles), and macro-scale rheometry (parallel-plate shear rheometer, open diamonds).

Table 1

The weight percentage of the crosslinker (bis-acrylamide) and monomer (acrylamide) used in the preparation of polyacrylamide gels

Sample	Weight% of crosslinker	Weight% of monomer
Low crosslinked gel	0.225	5
High crosslinked gel	0.264	8

Table 2

The Young's moduli of the hydrogels estimated from Hertz and JKR fits to the approach and retraction curves respectively, effective work of adhesion and the corresponding Tabor parameters are obtained from the pull-off forces measured by the fitting the JKR model to the retraction curve until zero depth of indentation

Sample	Hertz fit to the approach curve (kPa)	JKR fit to the retraction curve (kPa)	Eff. work of adhesion (mJ m^{-2})	Tabor parameter
High crosslinked gel	16.6 ± 0.9	14.6 ± 0.8	0.69 ± 0.11	150
Low crosslinked gel	8.1 ± 0.4	6.02 ± 0.8	0.75 ± 0.09	200